# The electrochemical behavior of $PbSO_4$ with different structures on Pb

Yonglang Guo [*], Lin Niu, Shuyong Zhang, Shenhao Chen

*Department of Chemistry, Shandong University, Jinan, 250100, China*

## Abstract

The reduction processes of $PbSO_4$ with different structures on Pb have been studied by the linear sweep voltammetry (LSV) and potential step technique. At high overpotential, the reduction rate of $PbSO_4$ depends on the diffusion of $SO_4^{2-}$ ions towards bulk solution and $Pb^{2+}$ ions towards the reaction surface. The large $PbSO_4$ crystals make the diffusion distance of $Pb^{2+}$ ions to the reaction surface extend, while the small $PbSO_4$ crystals impede the diffusion of $SO_4^{2-}$ ions through the micropores. The accumulation of $PbSO_4$ without activity occurs in the anodic film. The effects of the $H_2SO_4$ concentration and temperature are also discussed. © 2000 Elsevier Science S.A. All rights reserved.

## 1. Introduction

When a Pb electrode is oxidized at a potential positive to the $Pb/PbSO_4$ equilibrium potential, a dense $PbSO_4$ layer is formed and passivates the electrode surface. The stability of the passive state depends on the structure of the $PbSO_4$ layer formed under different conditions [1,2]. Many researchers believe that the dissolution/precipitation processes take place in the charge/discharge of the negative plate [3–5]. Since the $PbSO_4$ dissolves into $Pb^{2+}$ and $SO_4^{2-}$ ions in its reduction, the mass transfer of these two kinds of ions or/and the reduction of $Pb^{2+}$ ions are the rate-determining steps in the $PbSO_4$ reduction. At a small overpotential, the nucleation and growth of metallic lead limits the reduction rate of $Pb^{2+}$ ions [5–8]. However, it becomes fast with the increase of the polarization overpotential so that the $PbSO_4$ reduction rate is controlled by the diffusion of $Pb^{2+}$ ions through the interfaces between Pb and $PbSO_4$ crystals and the diffusion of $SO_4^{2-}$ ions in the micropores [9,10]. Therefore, the structure of $PbSO_4$ layer plays an important role in the mass transport of ions and its reduction.

Although the lead acid battery has been widely investigated, the research on the negative electrode is much less than that on the positive electrode. With the development of the valve-regulated lead acid (VRLA) battery and the

improvement of the battery performance, especially the cold cranking ability (CCA), more attention has been paid to the negative electrode recently [1–12]. In VRLA batteries, the big crystals of $PbSO_4$ may be formed by the chemical reduction of oxygen at negative plate. And the structures of $PbSO_4$ crystals formed are quite different under different discharge-rates and at different temperatures. Therefore, the effects of the $PbSO_4$ structure on its reduction have been studied in this work.

## 2. Experimental

The working electrode was a 99.999% lead cylinder of diameter 0.55 cm, which was press-fitted into a Teflon holder. An inclined plane of 45° was cut off and the exposed geometric area was 0.336 cm². The 2.5, 1, 0.5, 0.125 M $H_2SO_4$ and 0.125 M $H_2SO_4$ + 0.375 M $Na_2SO_4$ were prepared from analytical reagent (AR) and tri-distilled water. The $Hg/Hg_2SO_4/0.5$ M $H_2SO_4$ reference electrode was used in a three-electrode cell. The hole of the Luggin capillary in the electrolytic cell was so small that the $H_2SO_4$ concentrations in both working electrode and reference electrode compartments remained unchanged [13]. And in different $H_2SO_4$ solutions, we neglected the liquid junction potential drop, which might exist between the opposite sides of the Luggin capillary tip. Before each experiment, the electrode was mechanically polished on the emery paper up to 1000 grit with some alcohol on it,

---

[*] Corresponding author

followed by a short chemical etch in 10% nitric acid and the galvanostatical polarization for 1 min at 1 mA cathodic current. The linear sweep voltammetry (LSV) and potential step were carried out by the usual electrochemical instrumentation [13], which was connected to HP34970A acquirer and IBM PC computer. The electrolyte cell was maintained in a thermostatic water bath at $30.0 \pm 0.1$ or $0 \pm 1°C$. The appearances of $PbSO_4$ layer were observed by the scanning electron microscope (s-520). And an X-ray diffractometer (Rigaku, D/MAX-rA) was used in the X-ray diffraction experiments.

## 3. Results and discussion

Fig. 1 shows the three linear sweep voltammograms of the first cycle between $-1500$ and $-700$ mV at 30°C in three different solutions. Peak $a$ and $b$ denote the formation of $PbSO_4$ and its reduction, respectively. We find that the very high peak $a$ is formed in the positive-going sweep while a very small peak $b$ appears in the backward sweep under different $H_2SO_4$ concentrations. As the $H_2SO_4$ concentration decreases, both peaks become smaller and smaller and their peak potentials shift strongly in the positive direction. The changes in both peak potentials are caused mainly by the $H_2SO_4$ concentration and can be explained by the Nernst equation. From the changes in the electric charge of both peaks, we can see that a lot of $PbSO_4$ crystals are not reduced in the negative-going sweep and still remain on the electrode surface. The lower the $H_2SO_4$ concentration is, the more serious the electrode passivation becomes.

When the Pb electrode sweeps in the potential range between $-1500$ and $-700$ mV, the anodic current is only the oxidation of Pb to $PbSO_4$ while the cathodic current includes the reduction of $PbSO_4$ and hydrogen evolution. We find from Fig. 1 that the rate of hydrogen evolution is
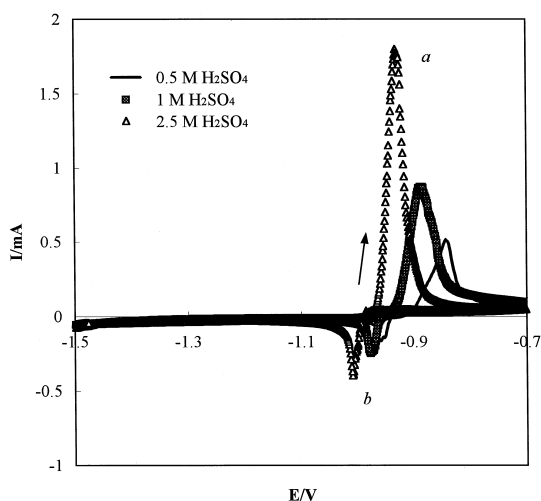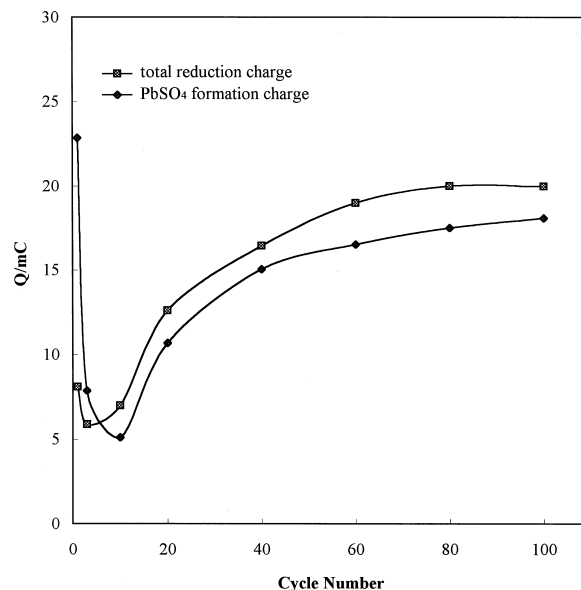


Fig. 2. The dependence of the electric charge on cycle number in 0.5 M $H_2SO_4$; potential sweep range: $-1500$ to $-700$ mV; sweep rate: 10 mV/s; temperature: 30°C.

very slow in the negative-going sweep. Fig. 2 shows the dependence of the $PbSO_4$ formation charge and total reduction charge in the range between $-1500$ and $-700$ mV on the cycle number in 0.5 M $H_2SO_4$. The similar results can also be obtained under other concentrations. We also notice that the electric charge of both oxidation and reduction decreases in the initial cycles and then increases gradually with the cycles. Although the evolution of hydrogen occurs simultaneously in the negative-going sweep, the total reduction charge is much smaller than the $PbSO_4$ formation charge in the initial cycles. It is clear that the accumulation of $PbSO_4$ occurs on the electrode surface. Since the porous anodic film thickens slowly in the subsequent cycles, these two kinds of charge increase gradually and then tend to be unchanged.

In order to study the influence of sweep rate on the $PbSO_4$ layer, we use a very slow sweep rate in the formation of $PbSO_4$, and its reduction peak under different $H_2SO_4$ concentrations is shown in Fig. 3. It is also observed that the reduction peak of $PbSO_4$ decreases with the decrease of the $H_2SO_4$ concentration.

Fig. 4 shows a series of LSVs of the 100th cycle at 30° and 0°C in two different solutions. Since the two kinds of electric charges in Fig. 2 tend to be unchanged after the 60th cycle, the LSVs in Fig. 4 can be considered as the stable LSVs under different conditions. All LSVs show that peak $b$ is much smaller than peak $a$ and most of the $PbSO_4$ is reduced in the following negative-going sweep. The lower the $H_2SO_4$ concentration is, the smaller peaks $a$ and $b$ are. The result is similar to the results in Fig. 1. When the temperature changes from 30° to 0°C, peaks $a$ and $b$ become very small, especially peak $b$, which almost disappears in Fig. 4B. It indicates that a serious passivation



Fig. 1. The 1st LSVs between $-1500$ and $-700$ mV under different $H_2SO_4$ concentrations on Pb; temperature: 30°C; sweep rate: 2 mV/s.
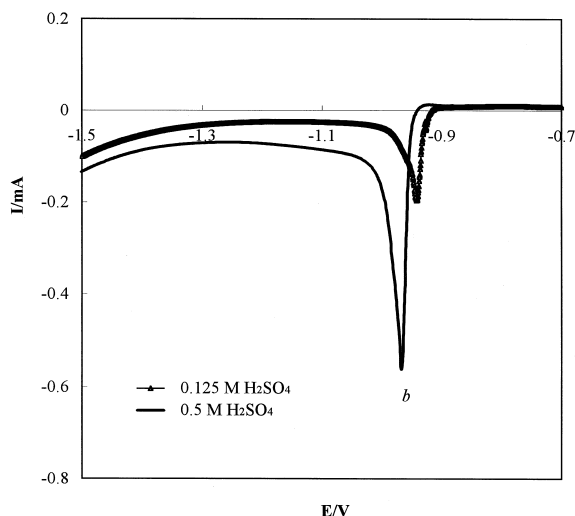
Fig. 3. The first cathodic LSVs at 2 mV/s under different $H_2SO_4$ concentrations on Pb when the $PbSO_4$ was formed in the anodic potential sweep at 0.1 mV/s; temperature: 30°C.

occurs on the electrode surface at low temperatures. This is because the $PbSO_4$ formed at low temperatures is difficult to reduce.

Fig. 5 shows the appearance of a $PbSO_4$ layer after the 100 cycles were performed under the conditions of Fig. 4. In comparison with Fig. 5A and B, the $PbSO_4$ crystals in Fig. 5C and D become smaller when the temperature decreases from 30° to 0°C. This is due to the slow transport rate of the ions at low temperatures. The reduction overpotential increases and small $PbSO_4$ crystals are formed. However, as the $H_2SO_4$ concentration decreases, the $PbSO_4$ crystals in Fig. 5B and D become larger, as compared with Fig. 5A and C, respectively. This is because low $H_2SO_4$ concentration can promote the dissolution of small crystals and the formation of large crystals. Since these large crystals are difficult to reduce, they accumulate on the electrode surface and passivate the electrode seriously.

Fig. 6 shows two typical LSVs. Two new peaks, peak $d$ and small peak $c$, are observed. Peak $d$ denotes the formation of $3PbO \cdot PbSO_4 \cdot H_2O$, which will be studied in another paper. Since the basic lead sulfates can be transformed into $PbSO_4$ easily in the negative-going sweep [14], the reduction peak of basic lead sulfates disappears and large $PbSO_4$ crystals can be formed by chemical transformation. According to the peak potential of peak $c$, only a reduction of $PbSO_4$ can exist in this potential range. Therefore, peak $c$ is most likely to denote the reduction of $PbSO_4$ with different structures, i.e., large $PbSO_4$ crystals. If the $H_2SO_4$ concentration increases, peak $c$ will become obscure or disappear. In comparison with the data in 0.5 M $H_2SO_4$ of Fig. 1, the higher reduction current is observed in the sweep negative to $-1000$ mV in Fig. 6. It shows that the reduction of many large $PbSO_4$ crystals occurs in this potential range. We find from Fig. 6 that peak $b$

becomes smaller and smaller with the decrease of the sweep rate, and almost all the $PbSO_4$ is reduced in the subsequent sweep at 2 mV/s. This is closely related to the large-$PbSO_4$-crystal structure formed in the anodic film.

Since the reduction current between $-1050$ and $-1500$ mV in Fig. 1 is very small, the hydrogen evolution is very slow at the polarization potential of $-1200$ mV. Fig. 7 shows three typical cathodic current–time curves when the potential steps from $-700$ to $-1200$ mV in 0.5, 1 and 2.5 M $H_2SO_4$. At first, the reduction current drops sharply, then the small current lasts for a long time. And quite extraordinarily, many random current peaks appear on the current–time curves. Because the hydrogen evolution rate is very small at $-1200$ mV, these small peaks should also be attributed to the reduction of $PbSO_4$ crystals. In the initial current decrease, the current is due to the reduction of the $PbSO_4$ crystals that are quite close to the reaction surface. After that, the remainder of the $PbSO_4$ crystals are so big and far from the lead surface that they are difficult to reduce, i.e., the remainder are the seriously passivated $PbSO_4$. However, when the passivated $PbSO_4$ is broken locally, dendrite lead grows and the large $PbSO_4$ crystals around it are reduced again. Thus, the current rises and small peaks appear once more. If the electrode surface is not seriously passivated, the small peaks in Fig. 7 become obscure or disappear (see Fig. 9). Fig. 8 shows an X-ray diffraction pattern obtained after the Pb electrode was polarized at $-1200$ mV for 1.5 h under the conditions of Fig. 7. Each diffraction line is pointed out by a $d$ value, which represents the distance between two crystal faces. Two large peaks without $d$ values are the Pb diffraction lines and the others are the $PbSO_4$ diffraction lines. Therefore, although the anodic film is reduced at $-1200$ mV for a very long time, many $PbSO_4$ crystals still remain on the
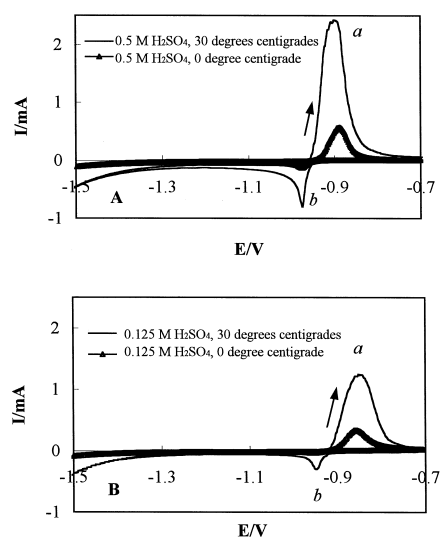


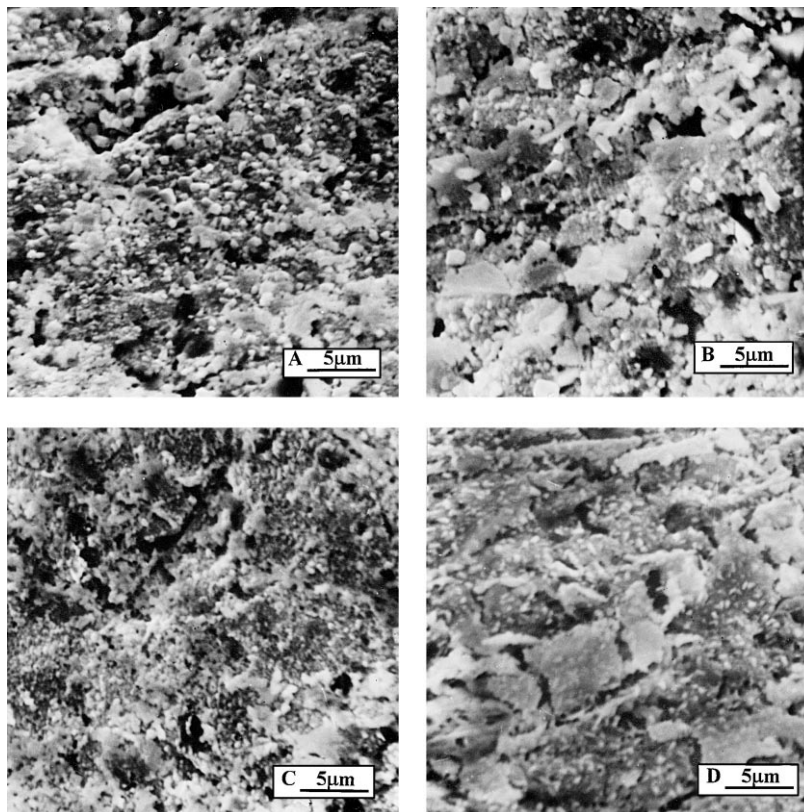Fig. 4. The 100th LSVs in different solutions on Pb at 30°C and 0°C, sweep rate: 10 mV/s.

Fig. 5. The appearances of $PbSO_4$ obtained under the conditions of Fig. 4; solutions: (A) and (C) 0.5 M $H_2SO_4$, (B) and (D) 0.125 M $H_2SO_4$; temperature: (A) and (B) 30°C, (C) and (D) 0°C.

electrode surface and small peaks in Fig. 7 are the reduction of these $PbSO_4$ crystals. It is clear that the activity of these crystals is very poor.

In order to analyze the behavior of peak $c$ in Fig. 6, the anodic film formed under the conditions of Fig. 6 was reduced at −1000 mV for 300 s and then the potential

stepped to −1200 mV. Fig. 9 shows the cathodic current–time curves at constant potentials in two different solutions. Since the electrode is polarized at −1000 mV during the initial period of 300 s, the falling current is due to the reduction of $PbSO_4$. At the beginning of the step to −1200 mV, the current decreases very slowly and it looks
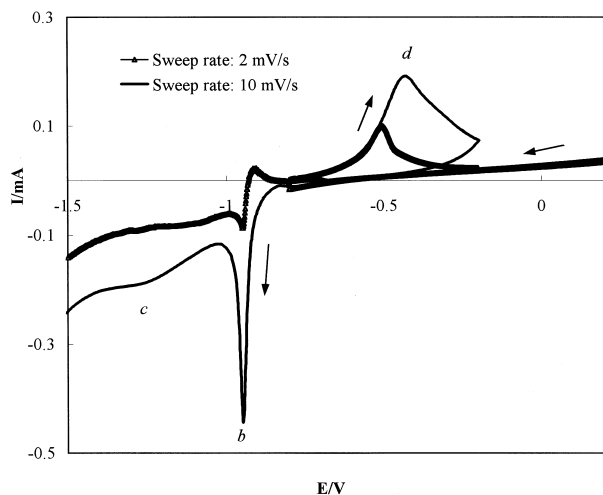


Fig. 6. The lead electrode was polarized at 200 mV for 15 min and the potential swept to −800 mV, followed by the sweep to −200 mV after the cathodic current dropped to zero at −800 mV and then swept back. Solution: 0.125 M $H_2SO_4$ + 0.375 M $Na_2SO_4$; temperature: 30°C.
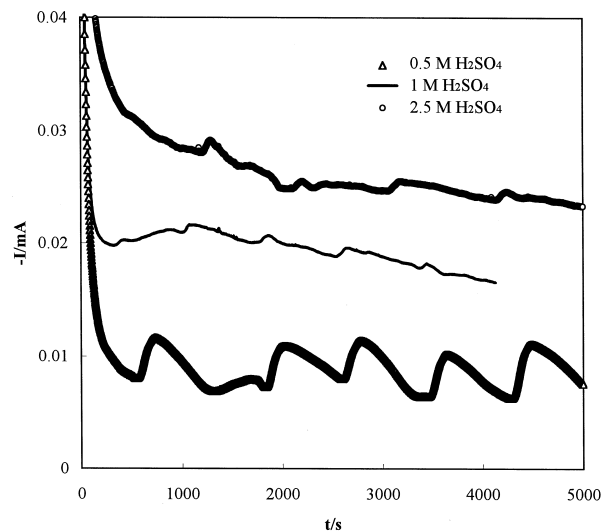


Fig. 7. The typical cathodic current–time curves when the Pb electrode was polarized at −700 mV for 15 min and then stepped to −1200 mV in different $H_2SO_4$ concentrations; temperature: 30°C.
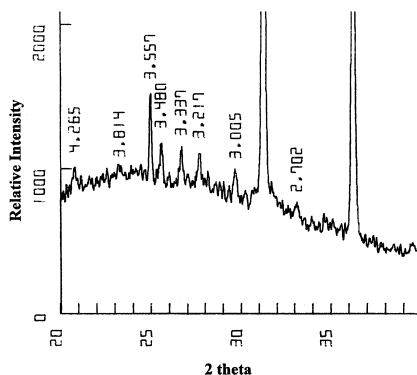
Fig. 8. The X-ray diffraction patterns when the Pb electrode was polarized at $-700$ mV for 15 min in 0.5 M $H_2SO_4$, followed by the potential step to $-1200$ mV and the polarization for 1.5 h; 40 kV, 50 mA.

as if an obscure peak appears, pointed out by the arrows. It is clear that a reduction reaction takes place at $-1200$ mV and corresponds to the reaction of peak $c$ in Fig. 6. Fig. 10 shows the dependence of the cathodic current ($I$) on the reciprocal of the square root of the step time ($t^{-0.5}$) at $-1200$ mV. We observe two straight-line relationships on each curve. So the reduction rate of peak $c$ is controlled by two kinds of processes. At short times, it looks as if the nucleation and growth including the diffusion process is a rate-determining step [6–8,15]. Since the polarization overpotential is very high, the current peak at about 400 s in Fig. 9 is very obscure. At long times, the straight-line relationship in Fig. 10 indicates that the reduction current is limited by the diffusion alone. Since the concentration of $Pb^{2+}$ ions is much lower than that of $SO_4^{2-}$ ions at the reaction interface, the diffusion of $Pb^{2+}$ ions from the $PbSO_4$ crystals to the reaction surface may be a limitation step.

Fig. 11 shows the dependence of $I$ on $t^{-0.5}$ obtained when the potential is stepped from $-700$ to $-1200$ mV.



Fig. 10. The dependence of the cathodic current on $t^{-0.5}$ after the potential step to $-1200$ mV as for Fig. 9.

Two straight-line relationships are obtained. Therefore, two kinds of diffusion processes can limit the reduction of the $PbSO_4$ layer. One may occur in the reduction of small $PbSO_4$ crystals at short times, another in the reduction of large $PbSO_4$ crystals at long times. At the beginning of the step, the low cathodic current may be caused by the nucleation and growth of metallic lead [6–8]. When the potential steps only to $-1100$ mV, the cathodic current is mainly the reduction of peak $b$ while almost no peak $c$ is reduced. Fig. 12 shows the dependence of $I$ on $t^{-0.5}$ obtained in the potential step to $-1100$ mV after different cycles. Only a straight-line relationship is obtained in different steps. It indicates that the diffusion process is a rate-determining step and the structure with even $PbSO_4$
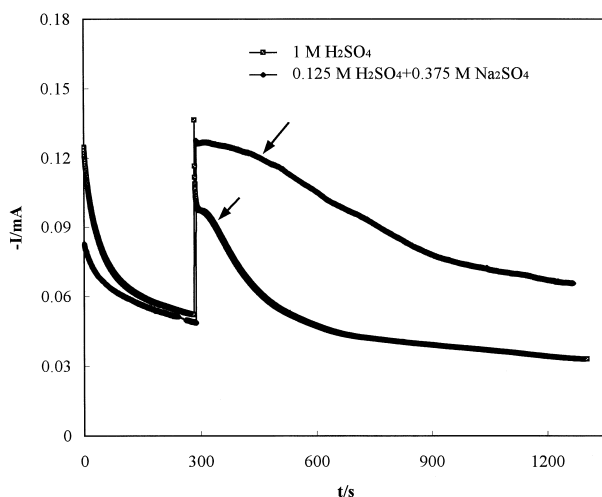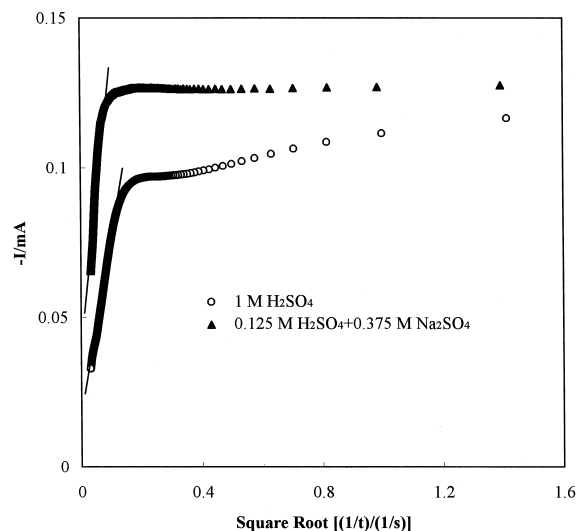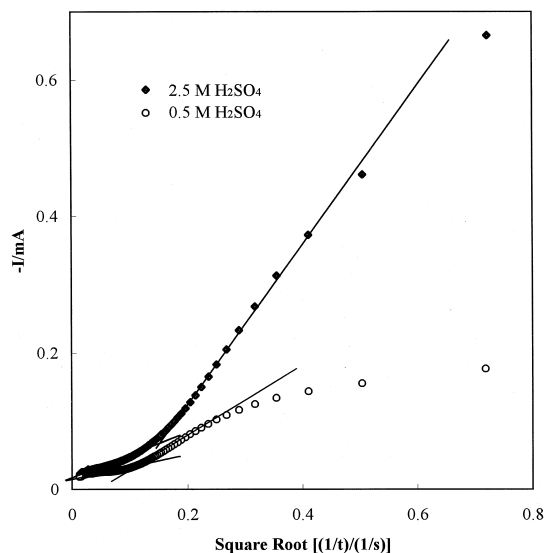


Fig. 9. The cathodic current–time curves obtained when the sweep potential arrived at $-1000$ mV under the conditions in Fig. 6, followed by a pause for 300 s and then steps to $-1200$ mV; temperature: 30°C.



Fig. 11. As for Fig. 7 but for the dependence of the cathodic current on $t^{-0.5}$ under different $H_2SO_4$ concentrations.
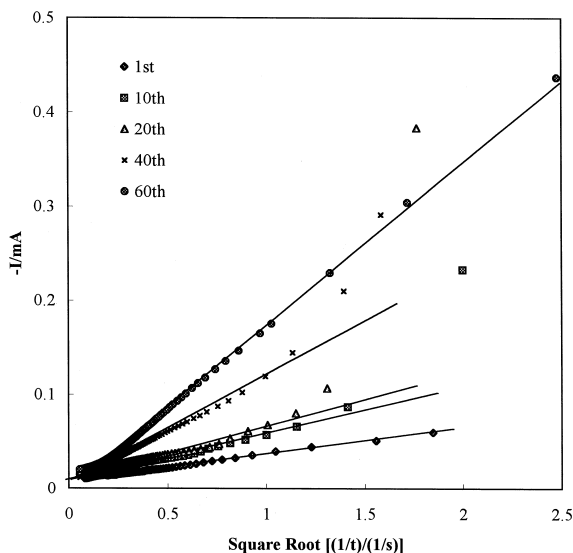
Fig. 12. The dependence of the cathodic current on $t^{-0.5}$ obtained by the potential step from $-900$ to $-1100$ mV when different cycles were carried out between $-1500$ and $-700$ mV at 10 mV/s; temperature: 30°C.

crystals is formed in the anodic film during the cycles. Since the slope of the straight line becomes bigger and bigger with the cycles, the $PbSO_4$ layer thickens constantly and its porosity increases during the cycles. At the beginning of the potential step, the cathodic current is very high. It is probable that the electrode is only slightly passivated and many nuclei still remain in the anodic film before the step. Therefore, the nucleation and growth of metallic lead and the ion diffusion near the reaction surface, rather than in the micropores, are very fast. After that, the reduction rate of $PbSO_4$ is controlled by the ion diffusion through the micropores in the anodic film.

## 4. Conclusion

In the reduction of $PbSO_4$, the $PbSO_4$ crystals dissolve into $Pb^{2+}$ and $SO_4^{2-}$ ions, followed by the diffusion of the $SO_4^{2-}$ ions towards bulk solution and the $Pb^{2+}$ ions towards the reaction surface at which the $Pb^{2+}$ ions get electrons and are reduced. Since the electron transfer is much faster than the mass transfer, both diffusions of $Pb^{2+}$ and $SO_4^{2-}$ ions are the rate-determining steps and depend upon the structure of $PbSO_4$ film. Yet, since the diffusion layer is very thin at the beginning of the reduction, the ion diffusion is very fast. Therefore, the nucleation and growth of metallic lead can also limit the reduction of $PbSO_4$.

During the oxidation, $PbSO_4$ crystals of different sizes can be formed under different conditions. In the cathodic polarization, small $PbSO_4$ crystals are reduced first and a high reduction current can be observed because of the short distance between $PbSO_4$ crystals and the reaction surface. The diffusion path of the ions extends constantly with the reduction of small $PbSO_4$ crystals. Meanwhile, when large $PbSO_4$ crystals are reduced, the distance of the ion diffusion from $PbSO_4$ crystals to the reaction surface becomes greater so that the rate of the $PbSO_4$ reduction is very slow and even the $PbSO_4$ crystals without activity accumulate in the anodic film. Since the concentration of $Pb^{2+}$ ions is much lower than that of $SO_4^{2-}$ ions, the transport of $Pb^{2+}$ ions is the rate-determining step. Therefore, two mechanisms controlled by the $Pb^{2+}$ diffusion exist in the reduction of different $PbSO_4$ crystals.

When the $H_2SO_4$ concentration decreases, the dissolution rate of small $PbSO_4$ crystals is fast. It promotes the growth of large $PbSO_4$ crystals that are difficult to reduce. Since the ion diffusion is very slow at low temperatures, the anodic overpotential increases and very small $PbSO_4$ crystals are formed in anodic film. Hence, the microporous passageways for the ion diffusion become narrow and long. The $SO_4^{2-}$ ion is difficult to diffuse from the bottom of the micropores to bulk solution. The electrode is seriously passivated. These two processes result in the accumulation of more $PbSO_4$ without activity in the anodic film. Therefore, only $PbSO_4$ with a certain structure can make both mass transfer of $Pb^{2+}$ and $SO_4^{2-}$ ions faster.

## Acknowledgements

## References

[1] D. Pavlov, R. Popova, Electrochim. Acta 15 (1970) 1483.
[2] D. Pavlov, Electrochim. Acta 13 (1968) 2051.
[3] J.R. Vilche, F.E. Varela, J. Power Sources 64 (1997) 39.
[4] K.R. Bullock, D. Pavlov (Eds.), Advances in lead-acid batteries, The Electrochemical Society, Pennington, NJ, 1984.
[5] G. Archdale, J.A. Harrison, J. Electroanal. Chem. 34 (1972) 21.
[6] N.A. Hampson, J.B. Lakeman, J. Electroanal. Chem. 107 (1980) 177.
[7] N.A. Hampson, J.B. Lakeman, J. Electroanal. Chem. 108 (1980) 347.
[8] F.E. Varela, L.M. Gassa, J.R. Vilche, Electrochim. Acta 37 (1992) 1119.
[9] K. Kanamura, Z. Takehara, J. Electrochem. Soc. 139 (1992) 345.
[10] Y. Guo, M. Wu, S. Hua, J. Power Sources 64 (1997) 65.
[11] F.E. Varela, L.M. Gassa, J.R. Vilche, J. Appl. Electrochem. 25 (1995) 358.
[12] P. Ekdunge, K.V. Rybalka, D. Simonsson, Electrochim. Acta 32 (1987) 659.
[13] Y. Guo, J. Electrochem. Soc. 138 (1991) 1222.
[14] Y. Guo, J. Electrochem. Soc. 140 (1993) 3369.
[15] Y. Guo, J. Electroanal. Chem. 345 (1993) 377.